Computational Materials Science 45 (2009) 756–761

Contents lists available at ScienceDirect

Computational Materials Science

journal homepage: www.elsevier.com/locate/commatsci

Crack growth modelling in single crystals based on higher order continua

Ozgur Aslan *, Samuel Forest

Centre des Matériaux, Mines ParisTech, UMR CNRS 7633, BP87, 91003 Evry Cedex, France

ARTICLE INFO

Article history:
Received 28 April 2008
Received in revised form 6 September 2008
Accepted 8 September 2008
Available online 26 October 2008

PACS:
81.40.Jj
81.40.Lm
81.40.Np
83.10.Ff
83.60.La

Keywords:
Damage regularization
Higher order continua
Damage mechanics
Softening
Localization
Cleavage
Micromorphic

ABSTRACT

This work presents several regularized crack growth models in brittle single crystals based on a combination of the micromorphic approach and continuum damage mechanics. First, a variant of micromorphic continuum, the microstrain theory, is chosen to explore the regularization capabilities of enhanced continua sparing three degrees of freedom compared to the full micromorphic approach. The difficulties in reaching final fracture of a sample are pointed out and an alternative damage criterion is proposed as a remedy which leads to a different localization pattern. Secondly, the microdamage formulation which enhances the numerical efficiency and also eliminates the final fracture difficulty is presented in detail. For all presented models, analytical solutions for governing differential equations are provided for 1D and the corresponding finite element simulation results are discussed.

1. Introduction

Conventional lifetime assessment models of crystalline solids are based on crack initiation criteria [1,2]. However, in the case of single crystals, anisotropic mechanical behaviour resulting from crystal structure and their general use in complex geometries (turbine industry) necessitates the consideration of crack growth [3]. In single crystals, crack initiation is generally triggered by complex thermomechanical loading conditions; therefore, the chosen constitutive model should satisfactorily describe the strongly anisotropic and nonlinear behaviour of single crystals under these various loading conditions.

After the significant work of Rice [4,5], the crystal plasticity theory has received great interest as a candidate to model crack growth in crystalline solids. In these works, growing cracks are associated to the crystallographic slip with a visco-plastic relation and the structure of the localization bands are linked to the slip systems. Especially in the field of fatigue, growing cracks and strain localization are mentioned together with the localization of plastic strain and damage.

In the literature, there are several modelling attempts which associate damage localization to crystallographic planes and inelastic deformations [6,7]. In this context, we focused on the continuum damage model for single crystals proposed by Marchal et al. [3]. In this model, three damage systems are associated to each {1 1 1} plane in FCC crystals. The first damage system is assigned as an opening system, activated by the normal stress, and mainly reflects a cleavage-like mechanism. The other two accommodate in plane deformations and enable arbitrary movements after fracture. The model allows for non straight crack paths and crack bifurcation. However, the model is identified for a given mesh size and type as in many damage models [8]. The mesh dependency arises from the loss of ellipticity of the continuum damage model after strong localization. Therefore, the boundary and initial value problems become ill-posed [9] and the numerical solution does not converge to a physically meaningful solution.

The main objective of this paper is to solve the above mentioned mesh dependency problem by exploring the regularization capabilities of the micromorphic theory applied to the continuum damage single crystal model. For that purpose, primarily, the continuous damage model developed by Marchal et al. is presented and simplified to concentrate on the regularization problem. In particular, the framework is limited to brittle cleavage fracture in

* Corresponding author.
E-mail address: ozgur.aslan@ensmp.fr (O. Aslan).

0927-0256/$ - see front matter © 2008 Elsevier B.V. All rights reserved.
doi:10.1016/j.commatsci.2008.09.016

single crystals with one single cleavage plane (suitable for instance for zinc single crystals). Two variants of the micromorphic continuum are considered. First, the microstrain theory [10] is applied, which introduces a microstrain tensor associated to each material point. Secondly, another variant of the micromorphic approach, microdamage model, is presented and its numerical capabilities as a powerful regularization technique are illustrated. Finally, several illustrative finite element results are presented in the last section. For simplicity, all theory and simulations are presented within the small strain framework.

2. Continuous damage model for single crystals

This model is based on the coupling between viscoplasticity and damage by introducing an additional damage strain variable $\dot{\underset{\sim}{\varepsilon}}^{\mathrm{d}}$, into the strain rate partition equation:

$$\dot{\underset{\sim}{\varepsilon}} = \dot{\underset{\sim}{\varepsilon}}^{\mathrm{e}} + \dot{\underset{\sim}{\varepsilon}}^{\mathrm{p}} + \dot{\underset{\sim}{\varepsilon}}^{\mathrm{d}} \tag{1}$$

where $\dot{\varepsilon}^{\mathrm{e}}$ and $\dot{\varepsilon}^{\mathrm{p}}$ are the elastic and the plastic strain rates, respectively. The damage strain $\dot{\underset{\sim}{\varepsilon}}^{\mathrm{d}}$ is decomposed in the following crystallographic contributions:

$$\dot{\underset{\sim}{\varepsilon}}^{\mathrm{d}} = \sum_{s=1}^{N_{\mathrm{planes}}^{\mathrm{d}}} \dot{\delta}^{\mathrm{s}} \underline{\boldsymbol{n}}^{\mathrm{s}} \otimes \underline{\boldsymbol{n}}^{\mathrm{s}} + \dot{\delta}_1^{\mathrm{s}} \underline{\boldsymbol{n}}^{\mathrm{s}} \overset{\mathrm{sym}}{\otimes} \underline{\boldsymbol{l}}_1^{\mathrm{s}} + \dot{\delta}_2^{\mathrm{s}} \underline{\boldsymbol{n}}^{\mathrm{s}} \overset{\mathrm{sym}}{\otimes} \underline{\boldsymbol{l}}_2^{\mathrm{s}} \tag{2}$$

where $\dot{\delta}^{\mathrm{s}}, \dot{\delta}_1^{\mathrm{s}}$ and $\dot{\delta}_2^{\mathrm{s}}$ are the strain rates for mode I, mode II and mode III crack growth, respectively and $N_{\mathrm{planes}}^{\mathrm{d}}$ stands for the number of damage planes which are fixed crystallographic planes depending on the crystal structure. Cleavage damage is represented by the opening δ^{s} of crystallographic cleavage planes with the normal vector $\underline{\boldsymbol{n}}^{\mathrm{s}}$ and other damage systems must be introduced for the in-plane accommodation along orthogonal directions $\underline{\boldsymbol{l}}_1^{\mathrm{s}}$ and $\underline{\boldsymbol{l}}_2^{\mathrm{s}}$, once cleavage has started (Fig. 1). Material separation is assumed to take place with respect to specific crystallographic planes, like cleavage planes in single crystals. Three damage criteria are associated to one cleavage and two accommodation systems:

$$f_{\mathrm{c}}^{\mathrm{s}} = |\underline{\boldsymbol{n}}^{\mathrm{s}} \cdot \underset{\sim}{\boldsymbol{\sigma}} \cdot \underline{\boldsymbol{n}}^{\mathrm{s}}| - Y^{\mathrm{s}} \tag{3}$$

$$f_i^{\mathrm{s}} = |\underline{\boldsymbol{n}}^{\mathrm{s}} \cdot \underset{\sim}{\boldsymbol{\sigma}} \cdot \underline{\boldsymbol{l}}_i^{\mathrm{s}}| - Y_i^{\mathrm{s}} \quad (i = 1, 2) \tag{4}$$

The critical normal stress Y^{s} for damage decreases as δ increases:

$$Y^{\mathrm{s}} = Y_0^{\mathrm{s}} + H\delta^{\mathrm{s}} \tag{5}$$

where Y_0^{s} is the initial damage stress (usually coupled to plasticity) and H is a negative modulus which controls material softening due to damage. Information regarding the evolution of the threshold Y_i^{s} can be found in [3] Finally, evolution of damage is given by the following equations;

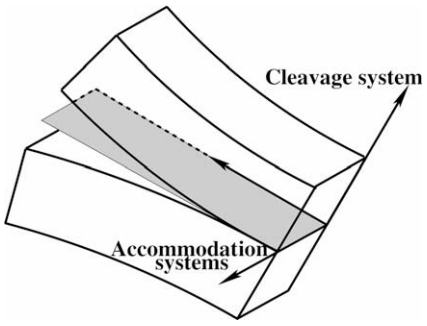

Fig. 1. Illustration of the cleavage and two accommodation systems to be associated to the crystallographic planes.

$$\dot{\delta}^{\mathrm{s}} = \left\langle \frac{f_{\mathrm{c}}^{\mathrm{s}}}{K_{\mathrm{d}}} \right\rangle^{n_{\mathrm{d}}} \mathrm{sign}\left(\underline{\boldsymbol{n}}^{\mathrm{s}} \cdot \underset{\sim}{\boldsymbol{\sigma}} \cdot \underline{\boldsymbol{n}}^{\mathrm{s}} \right) \tag{6}$$

$$\dot{\delta}_i^{\mathrm{s}} = \left\langle \frac{f_i^{\mathrm{s}}}{K_{\mathrm{d}}} \right\rangle^{n_{\mathrm{d}}} \mathrm{sign}\left(\underline{\boldsymbol{n}}^{\mathrm{s}} \cdot \underset{\sim}{\boldsymbol{\sigma}} \cdot \underline{\boldsymbol{l}}_i^{\mathrm{s}} \right) \tag{7}$$

where K_{d} and n_{d} are material parameters.

These equations hold for all conditions except when the crack is closed ($\delta^{\mathrm{s}} < 0$) and compressive forces are applied ($\underline{\boldsymbol{n}}^{\mathrm{s}} \cdot \underset{\sim}{\boldsymbol{\sigma}} \cdot \underline{\boldsymbol{n}}^{\mathrm{s}} < 0$). In this case, damage evolution stops ($\dot{\delta}^{\mathrm{s}} = \dot{\delta}_i^{\mathrm{s}} = 0$), corresponding to the unilateral damage conditions.

This model, complemented by the suitable constitutive equations for viscoplastic strain, has been used for the simulation of crack growth under complex cyclic loading at high temperature [11]. Significant mesh dependency of results was found [12]. In the present work, the model is simplified and reduced to brittle "cleavage-like" damage behaviour in single crystals by considering only one single cleavage plane. The objective is to assess the regularization capabilities of two higher order extensions of the single crystal damage model.

3. Microstrain continuum

The micromorphic medium introduced by Eringen and Suhubi [13] possesses a full microdeformation field χ, in addition to the classical displacement field $\underline{\boldsymbol{u}}$. Containing additional degrees of freedom and balance equations, the micromorphic continuum approach can be considered as the main framework for most generalized continuum models [14]. If one introduces a symmetric tensor by disregarding the skew–symmetric part of the microdeformation, the theory decays into the microstrain model [10].

3.1. Balance and constitutive equations

A symmetric microstrain tensor ${}^{\chi}\underset{\sim}{\boldsymbol{\varepsilon}}$ associated with the macrostrain $\underset{\sim}{\boldsymbol{\varepsilon}}$ is introduced and considered as a degree of freedom (DOF) in addition to the displacement vector $\underline{\boldsymbol{u}}$:

$$\mathrm{DOF} = \{\underline{\boldsymbol{u}}, {}^{\chi}\underset{\sim}{\boldsymbol{\varepsilon}}\} \tag{8}$$

Generalized strain measures can be defined as the strain, relative deformation and gradient of micro-deformation tensors respectively:

$$\underset{\sim}{\boldsymbol{\varepsilon}} = \underline{\boldsymbol{u}} \overset{\mathrm{sym}}{\otimes} \boldsymbol{\nabla}, \quad \underset{\sim}{\boldsymbol{e}} = \underset{\sim}{\boldsymbol{\varepsilon}} - {}^{\chi}\underset{\sim}{\boldsymbol{\varepsilon}}, \quad \underset{\approx}{\boldsymbol{K}} = {}^{\chi}\underset{\sim}{\boldsymbol{\varepsilon}} \otimes \boldsymbol{\nabla} \tag{9}$$

The symmetric part of the displacement gradient is denoted by $\underline{\boldsymbol{u}} \overset{\mathrm{sym}}{\otimes} \boldsymbol{\nabla}$. The symmetric force stress tensor $\boldsymbol{\sigma}$, the relative stress tensor $\boldsymbol{s}$ and a third order stress tensor $\underset{\approx}{\boldsymbol{S}}$ are associated with these strain measures in the work of internal forces. The following balance of momentum and balance of moment of momentum equations must be fulfilled:

$$\left(\underset{\sim}{\boldsymbol{\sigma}} + \underset{\sim}{\boldsymbol{s}} \right) . \boldsymbol{\nabla} = 0 \tag{10}$$

$$\underset{\approx}{\boldsymbol{S}} . \boldsymbol{\nabla} + \underset{\sim}{\boldsymbol{s}} = 0 \tag{11}$$

where $\cdot\boldsymbol{\nabla}$ represents the divergence operator. These equations are coupled by relative stress tensor $\boldsymbol{s}$. The boundary conditions for the traction vector $\underline{\boldsymbol{t}}$ and double traction tensor $\underset{\sim}{\boldsymbol{M}}$ read:

$$\underline{\boldsymbol{t}} = \left(\underset{\sim}{\boldsymbol{\sigma}} + \underset{\sim}{\boldsymbol{s}} \right) . \underline{\boldsymbol{n}}, \quad \underset{\approx}{\boldsymbol{M}} = \underset{\approx}{\boldsymbol{S}} . \underline{\boldsymbol{n}} \tag{12}$$

Elasticity relations are of the form:

$$\underset{\sim}{\boldsymbol{\sigma}} = \underset{\approx}{\boldsymbol{c}} : \underset{\sim}{\boldsymbol{\varepsilon}}^{\mathrm{e}}, \quad \underset{\sim}{\boldsymbol{s}} = \underset{\approx}{\boldsymbol{b}} : \underset{\sim}{\boldsymbol{e}}, \quad \underset{\approx}{\boldsymbol{S}} = \underset{\approx\approx}{\boldsymbol{A}} \vdots \underset{\approx}{\boldsymbol{K}} \tag{13}$$

In this work, only the symmetric strain tensor is decomposed into elastic and damage parts for the sake of simplicity.

$$\underset{\sim}{\boldsymbol{\varepsilon}} = \underset{\sim}{\boldsymbol{\varepsilon}}^{\mathrm{e}} + \underset{\sim}{\boldsymbol{\varepsilon}}^{\mathrm{d}} \tag{14}$$

Considering only cleavage, the evolution equation is derived from the yield function f_c using normality, such as:

$$\dot{\underset{\sim}{\boldsymbol{\varepsilon}}}^{\mathrm{d}} = \dot{\delta}\frac{\partial f_c}{\partial \underset{\sim}{\boldsymbol{\sigma}}} \tag{15}$$

For the localization analysis, softening rule (5) and damage criteria (3) are used.

3.2. Application to 1D problem

For the 1D problem, a bar with length L under tension is analyzed (Fig. 2). For the analysis, a vanishing Poisson ratio is taken and elastic tensors $\underset{\approx}{\boldsymbol{c}}$ and $\underset{\approx}{\boldsymbol{b}}$ are assumed equal. Viscosity is excluded from the solutions and the cleavage plane is normal to direction two. For the damage threshold function, two different cases are investigated. First, the yield function which is controlled by the normal stress $|\underline{\boldsymbol{n}}\cdot\underset{\sim}{\boldsymbol{\sigma}}\cdot\underline{\boldsymbol{n}}|$ is studied and a comparison between analytical and numerical results is drawn. As a second case, the yield function is modified by introducing the relative stress tensor in addition to the Cauchy stress.

3.2.1. Classical linear softening

Recalling the Eq. (5), one can write the classical linear yield function in a complete form for 1D as:

$$f_c = |\sigma_{22}| - (Y_0 + H\delta) \tag{16}$$

From the consistency condition of the yield function, $\dot{f}_c = 0, \dot{\delta}$ can be solved as:

$$\dot{\delta} = \frac{2\mu(\dot{\varepsilon}_{22} - \dot{\varepsilon}^{\mathrm{d}}_{22})}{H} \tag{17}$$

where μ is the second Lamé constant. Inserting (15) into the above equation:

$$\dot{\delta} = \frac{2\mu\dot{\varepsilon}_{22}}{2\mu + H} \tag{18}$$

and for monotonic loading one gets:

$$\delta = \frac{2\mu}{2\mu + H}\left(\varepsilon_{22} - \frac{Y_0}{2\mu}\right) \tag{19}$$

The balance Eqs. (10) and (11) must be taken into account for the analytical solution:

$$\sigma_{22,2} + s_{22,2} = 0, \quad S_{222,2} + s_{22} = 0 \tag{20}$$

$$\sigma_{22} = 2\mu(\varepsilon_{22} - \varepsilon^{\mathrm{d}}_{22}) = \frac{2\mu}{2\mu + H}(H\varepsilon_{22} + Y_0) \tag{21}$$

$$s_{22} = 2\mu(\varepsilon_{22} - {}^{\chi}\varepsilon_{22}), S_{222} = A^{\chi}\varepsilon_{22,2} \tag{22}$$

and a system of equations is obtained for the unknowns $\varepsilon_{22,2}$ and ${}^{\chi}\varepsilon_{22,2}$ which can be solved for boundary conditions (12):

$$\overline{H}\varepsilon_{22,2} + 2\mu(\varepsilon_{22,2} - {}^{\chi}\varepsilon_{22,2}) = 0, \tag{23}$$

$$A^{\chi}\varepsilon_{22,22} + 2\mu(\varepsilon_{22} - {}^{\chi}\varepsilon_{22}) = 0 \tag{24}$$

where $\overline{H} = 2\mu H/(2\mu + H)$. The strain component ε_{22} can be eliminated from the previous system to get:

$${}^{\chi}\varepsilon_{22,222} - \frac{2\mu\overline{H}}{A(\overline{H} + 2\mu)}{}^{\chi}\varepsilon_{22,2} = 0 \tag{25}$$

When H is negative and $\overline{H} + 2\mu$ remains positive, the solution is sinusoidal:

$${}^{\chi}\varepsilon_{22} = \alpha\sin(\omega x_2) + \beta\cos(\omega x_2) + \gamma \tag{26}$$

with a wave length:

$$\frac{2\pi}{\omega} = 2\pi\sqrt{\frac{A(H + \mu)}{\mu H}} \tag{27}$$

Finally, solving (23) and (24) for ε_{22} and inserting it into (19), the crack opening δ is found to read:

$$\delta = \frac{1}{2\mu + H}[(2\mu - A\omega^2){}^{\chi}\varepsilon_{22} - A\omega^2\gamma - Y_0] \tag{28}$$

From Fig. 3, it is concluded that the damage is regularized throughout the rod and the computations are perfectly matching with the analytical solution. However, the model exhibits an inability to soften up to final fracture (Fig. 7). This is due to the divergence contribution of the higher order stress $\underset{\approx}{\boldsymbol{S}}$ to the relative stress $\underset{\sim}{\boldsymbol{s}}$ as it is postulated in the balance Eq. (11). As long as there exists gradient of $\underset{\approx}{\boldsymbol{S}}$, the complement relative stress remains. Since the traction vector on the cleavage plane is related to $\sigma_{22} + s_{22}$, it cannot vanish even for ever-increasing crack opening. This shortcoming is also mentioned by Engelen et al. in the context of gradient enhanced approach for softening [15].

As a remedy, a coupling between the force stress $\underset{\sim}{\boldsymbol{\sigma}}$ and the relative stress $\underset{\sim}{\boldsymbol{s}}$ must be introduced into the yield function in order to achieve a total softening in the whole stress space, as investigated in the next subsection.

3.2.2. Modified damage threshold function

The damage threshold function (3) is modified so as to incorporate the effective stress $\underset{\sim}{\boldsymbol{\sigma}} + \underset{\sim}{\boldsymbol{s}}$:

$$f_c = \left|\underline{\boldsymbol{n}}\cdot\left(\underset{\sim}{\boldsymbol{\sigma}} + \underset{\sim}{\boldsymbol{s}}\right)\cdot\underline{\boldsymbol{n}}\right| - Y \tag{29}$$

Similar to the first case, for monotonic loading, one gets:

$$\delta = \frac{2\mu}{2\mu + H}\left(2\varepsilon_{22} - \frac{Y_0}{2\mu} - {}^{\chi}\varepsilon_{22}\right) \tag{30}$$

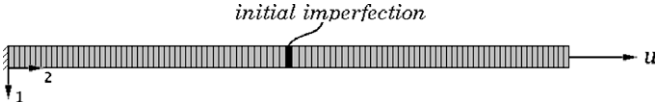

Fig. 2. 1D rod under tension with an initial imperfection.

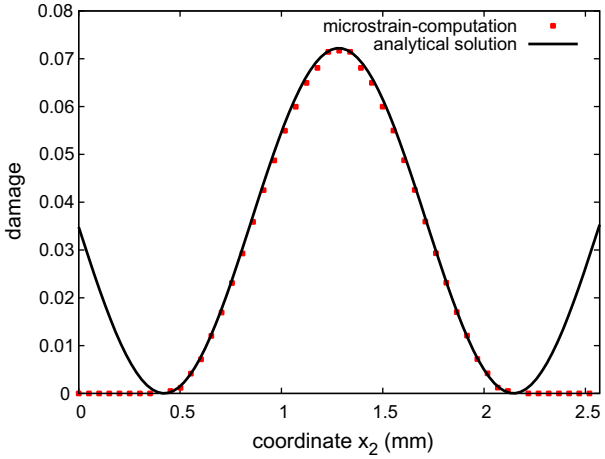

Fig. 3. Comparison between numerical and analytical solution of a 1D rod under uniaxial tension with a central initial defect for linear softening. The analytical solution holds for the damaged zone and the rest of the rod behaves purely elastically ($A = 30$ MPa mm^2, $H = 400$ MPa, $\mu = 200000$ MPa).

and stress terms read:

$$\sigma_{22} = \frac{2\mu}{2\mu + H}[(H - 2\mu)\varepsilon_{22} + 2\mu^{\chi}\varepsilon_{22} + Y_0] \tag{31}$$

$$s_{22} = 2\mu(\varepsilon_{22} - {}^{\chi}\varepsilon_{22}), S_{222} = A^{\chi}\varepsilon_{22,2} \tag{32}$$

Writing the first balance Eq. (10) and taking the derivative with respect to the second coordinate one gets:

$$\sigma_{22,2} + s_{22,2} = 0 \tag{33}$$

$$2\mu(\varepsilon_{22,2} - {}^{\chi}\varepsilon_{22,2}) + \frac{2\mu}{2\mu + H}[(H - 2\mu)\varepsilon_{22,2} + 2\mu^{\chi}\varepsilon_{22,2}] = 0 \tag{34}$$

which reduces to the following relation:

$$\varepsilon_{22,2} = \frac{1}{2}{}^{\chi}\varepsilon_{22,2} \tag{35}$$

Rewriting the second balance Eq. (11) and taking the derivative, the following additional relation is obtained:

$$A^{\chi}\varepsilon_{22,222} + 2\mu(\varepsilon_{22,2} - {}^{\chi}\varepsilon_{22,2}) = 0 \tag{36}$$

Inserting now (35) into (36) gives:

$$A^{\chi}\varepsilon_{22,222} - \mu^{\chi}\varepsilon_{22,2} = 0 \tag{37}$$

The general solution can be written in terms of hyperbolic functions, such as:

$${}^{\chi}\varepsilon_{22} = \alpha\sinh(\omega x_2) + \beta\cosh(\omega x_2) + \gamma \tag{38}$$

with the wave length

$$\frac{2\pi}{\omega} = 2\pi\sqrt{\frac{A}{\mu}} \tag{39}$$

which is independent of H and acts as a length scale for the model.

Note that this solution holds for each side of the defective zone. Furthermore, the analytical solution for ε_{22} is of the same kind with different constants such that

$$\varepsilon_{22} = C_1\sinh(\omega x_2) + C_2\cosh(\omega x_2) + C_3 \tag{40}$$

where $C_1 = 2\alpha, C_2 = 2\beta$ and $C_3 = \gamma$. γ is nothing but the elastic strain outside the damaged part of the rod, $Y_0/2\mu$ and other constants can be solved by taking $S_{22} = 0$ at $x_2 = 0$ and $x_2 = l$.

Fig. 6 shows that the present model is able to describe final fracture of the bar. However, if we take the derivative of (30) and insert (35) into it, the derivative of damage variable, δ, with respect to the second coordinate, is shown to vanish. This means that damage becomes piecewise constant throughout the bar and the damage distribution is trapped into the element which has the imperfection as it is illustrated in Fig. 5. Nevertheless, micro and macro strain still possesses the hyperbolic distribution (Fig. 4). As a result, this variant of the microstrain model is not satisfying.

In general, the higher order stress tensor $\boldsymbol{S}$ could also enter the yield condition (3). Keeping the normality rule implies that elastic and plastic parts should be considered for the microstrain χ and the microstrain gradient $\boldsymbol{K}$. This track, although possible, is not pursued here (see [16,17]).

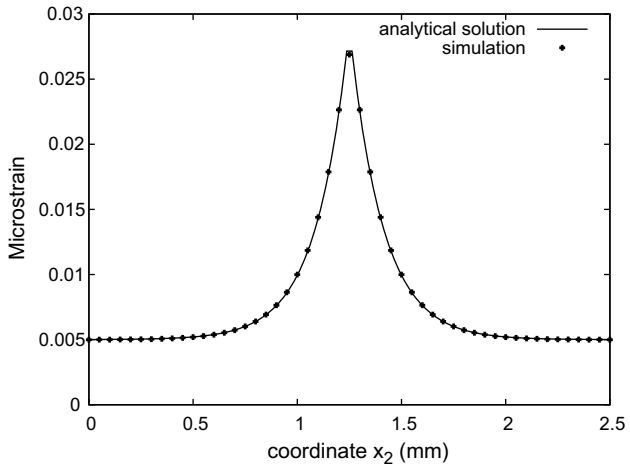

Fig. 4. Comparison between numerical and analytical solution of a 1D rod under uniaxial tension with a central initial defect with modified damage threshold ($A = 2500$ MPa mm^2, $H = 1$ MPa, $\mu = 200\,000$ MPa).

4. Microdamage continuum

Alternative micromorphic variables other than the full strain tensor can be chosen [14]. The strain gradient effect can be limited to the damage strain $\boldsymbol{\varepsilon}^{\mathrm{d}}$ gradient and more specifically to δ in the case of a single damage system.

4.1. Balance and constitutive equations

In this microdamage theory, the selected microvariable is a scalar microdamage parameter ${}^{\chi}\delta$ instead of a microstrain tensor, which reduces the number of additional degrees of freedom to one and provides improved efficiency in computations:

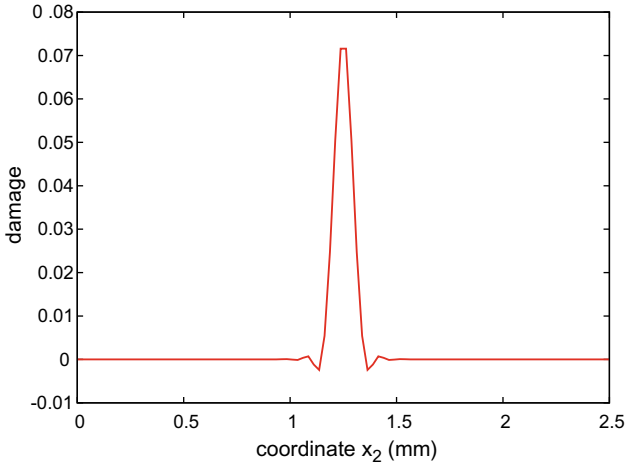

Fig. 5. Damage distribution along the rod for the modified damage threshold. Note that damage is trapped in the imperfection zone.

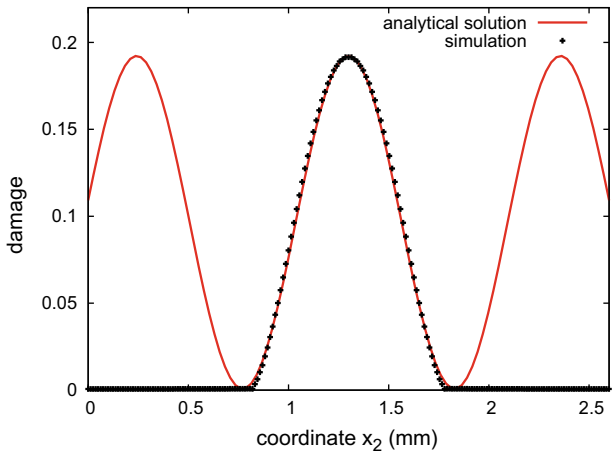

Fig. 6. Comparison between force vs. displacement diagram of a 1D softening rod for microstrain and microdamage continua.

$$\text{DOF} = \{\underline{\boldsymbol{u}}, {}^{\chi}\delta\} \quad \text{Strain} = \{\varepsilon, {}^{\chi}\delta, \nabla{}^{\chi}\delta\} \tag{41}$$

The power of internal forces is extended as

$$p^{(i)} = \underset{\sim}{\boldsymbol{\sigma}} : \underset{\sim}{\dot{\boldsymbol{\varepsilon}}} + a\,{}^{\chi}\dot{\delta} + \underline{\boldsymbol{b}}.\nabla{}^{\chi}\dot{\delta} \tag{42}$$

where generalized stresses $a, \underline{\boldsymbol{b}}$ have been introduced. The generalized balance equations are:

$$\operatorname{div} \underset{\sim}{\boldsymbol{\sigma}} = 0, \quad a = \operatorname{div}\underline{\boldsymbol{b}} \tag{43}$$

The free energy density is taken as a quadratic potential in the elastic strain, damage δ, relative damage $\delta - {}^{\chi}\delta$ and microdamage gradient $\nabla{}^{\chi}\delta$:

$$\rho\psi = \frac{1}{2}\underset{\sim}{\boldsymbol{\varepsilon}}^{e} : \underset{\approx}{\boldsymbol{c}} : \underset{\sim}{\boldsymbol{\varepsilon}}^{e} + \frac{1}{2}H\delta^2 + \frac{1}{2}{}^{\chi}H(\delta - {}^{\chi}\delta)^2 + \frac{1}{2}A\nabla{}^{\chi}\delta\nabla{}^{\chi}\delta \tag{44}$$

where $H, {}^{\chi}H$ and A are scalar material constants. Then, the elastic response of the material becomes:

$$\underset{\sim}{\boldsymbol{\sigma}} = \rho\frac{\partial\psi}{\partial\underset{\sim}{\boldsymbol{\varepsilon}}^{e}} = \underset{\approx}{\boldsymbol{c}} : \underset{\sim}{\boldsymbol{\varepsilon}}^{e} \tag{45}$$

The generalized stresses read:

$$a = \rho\frac{\partial\psi}{\partial{}^{\chi}\delta} = -{}^{\chi}H(\delta - {}^{\chi}\delta), \underline{\boldsymbol{b}} = A\nabla{}^{\chi}\delta \tag{46}$$

and the driving force for damage can be derived as:

$$Y = \rho\frac{\partial\psi}{\partial\delta} = d(H + {}^{\chi}H) - {}^{\chi}H{}^{\chi}\delta \tag{47}$$

The damage criterion now is:

$$f = \left|\underline{\boldsymbol{n}}^{s} \cdot \underset{\sim}{\boldsymbol{\sigma}} \cdot \underline{\boldsymbol{n}}^{s}\right| - Y_0 - Y = 0 \tag{48}$$

where Y_0 is the initial threshold value for damage activation. Substituting the linear constitutive equations for generalized stresses into the additional balance Eq. (43), assuming homogeneous material properties, leads to the following partial differential equation for the microdamage

$${}^{\chi}\delta - \frac{A}{{}^{\chi}H}\Delta{}^{\chi}\delta = \delta \tag{49}$$

where the macrodamage δ acts as a source term. Exactly this type of Helmholtz equation has been postulated in the so–called implicit gradient theory of plasticity and damage [18,15,19,20], where the microvariables are called non local variables and where the generalized stresses a and $\underline{\boldsymbol{b}}$ are not explicitly introduced (see [14,21] for the analogy between this latter approach and the micromorphic theory).

4.2. Solution for 1D bar

The damage function can be rewritten for the 1D-rod case as follows:

$$f = 2\mu(\varepsilon_{22} - \delta) - Y_0 - (H + {}^{\chi}H)\delta + {}^{\chi}H{}^{\chi}\delta = 0 \tag{50}$$

The system of equations to be solved for $\underset{\sim}{\boldsymbol{\varepsilon}}, d$ and ${}^{\chi}d$ reads:

$$\sigma_{22,2} = 2\mu(\varepsilon_{22,2} - \delta_{,2}) = 0 \tag{51}$$

$$A{}^{\chi}\delta_{,22} + {}^{\chi}H(\delta - {}^{\chi}\delta) = 0 \tag{52}$$

Due to the Eq. (51), taking the derivative of (50) with respect to the second coordinate gives

$$-\delta_{,2}(H + {}^{\chi}H) + {}^{\chi}H{}^{\chi}\delta_{,2} = 0 \tag{53}$$

Taking the derivative of (52) with respect to the second coordinate and inserting (53) into (52) gives:

$${}^{\chi}\delta_{,222} = \frac{{}^{\chi}HH}{A(H + {}^{\chi}H)}{}^{\chi}\delta_{,2} \tag{54}$$

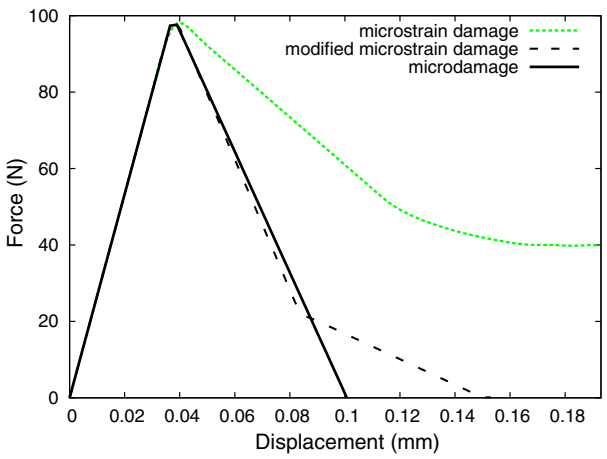

Fig. 7. Comparison between numerical and analytical solutions of a 1D rod under tension for microdamage continuum. The analytical solution is only valid at the damage zone, the rest undergoes elastic unloading ($A = 200$ MPa mm^2, $H = -16000$ MPa, ${}^{\chi}H = 50000$ MPa, $\mu = 200000$ MPa).

It appears that when $\frac{H{}^{\chi}H}{H+{}^{\chi}H} < 0$, the solution for ${}^{\chi}\delta$ is sinusoidal:

$${}^{\chi}\delta = \alpha\sin(\omega x_2) + \beta\cos(\omega x_2) + \gamma \tag{55}$$

where $\omega = \sqrt{|H{}^{\chi}H/A(H + {}^{\chi}H)|}$. Same solution also holds for ε and δ with different constants as shown in Fig. 7.

In comparison with the microstrain approach, the microdamage theory eliminates the final fracture problem without any modification since there exists no direct coupling between force stress $\underset{\sim}{\boldsymbol{\sigma}}$

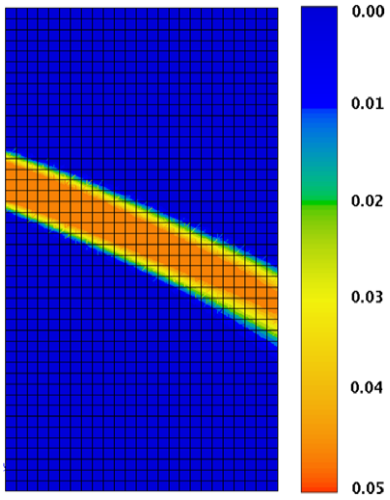

Fig. 8. Crack propagating through a 2D single crystal block with a single inclined cleavage plane under vertical tension with 8% strain. Field variable δ.

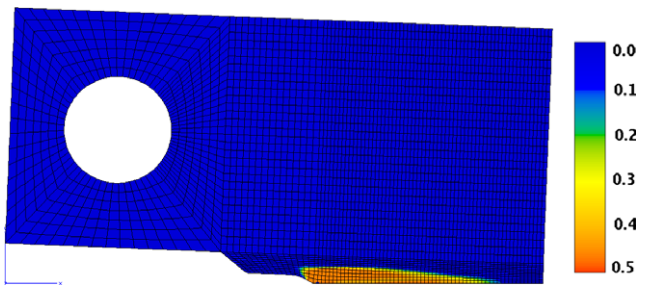

Fig. 9. Crack growth in a CT-like specimen under tension. Field variable δ.

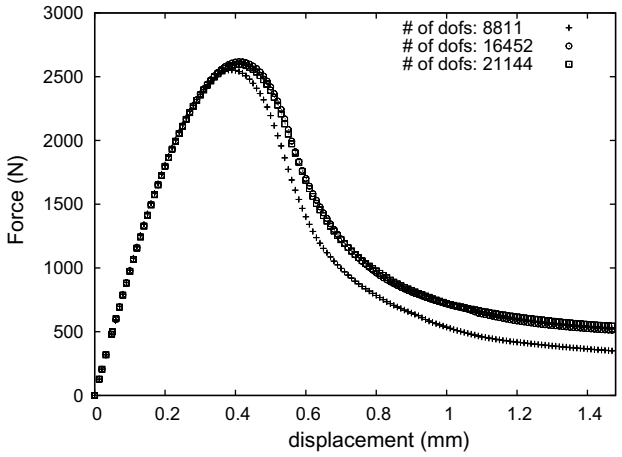

Fig. 10. Mesh independency of the numerical solution for the CT-like specimen demonstrated in Fig. 9; force vs. displacement diagrams for an increasing number of total degrees of freedom.

and generalized stresses. It provides consistent crack growth on the cleavage plane with various orientation (Fig. 8 for an inclined cleavage plane with respect to the load axis).

5. Examples

In this section several FE analyses performed by microdamage theory are demonstrated.

As a 2D example, a plate under uniaxial tension with an inclined cleavage plane is investigated (Fig. 8). In order to trigger localization, an initial geometric defect is created on the left edge and the cleavage plane is oriented at 30 degrees from the horizontal axis. FEA results show that localization path is perfectly matching with the cleavage plane and the size of the localization band is controlled by ω in (55).

In Fig. 9, FEA of a CT-like fracture mechanics specimen under tension is considered [5]. The analysis is done by creating a cleavage plane parallel to the horizontal axis and the loading is performed from the center of the pin. For a given characteristic length (associated with parameters $A = 200\,\text{MPa mm}^2, H = -16\,000\,\text{MPa}, \chi H = 50\,000\,\text{MPa}$), mesh refinement of the specimen leads to a unique fracture curve and a finite size crack width, as shown in Figs. 9 and 10.

6. Conclusion

Three variants of micromorphic continuum and their regularization capabilities for the modelling of crack propagation in single crystals have been scrutinized. First, a crystallographic constitutive model which accounts for continuum damage with respect to fracture planes has been presented. Then, the theory has been extended from classical continuum to microstrain and microdamage continua, respectively. It has been shown that both approaches can be good candidates in solving mesh dependency and, under circumstances, the prediction of final fracture. Analytical fits and numerical results showed that both theories are well suited for FEA and possess great potential for the future modelling aspects.

The issues to be considered in the future are the proper choice of the best–suited elements (interpolation functions in particular) and the coupling with crystal plasticity. Comparison with available data on crack growth in single crystals, especially cyclic loading in nickel–based superalloys, will be decisive to conclude on the ability of such generalized continuum damage approaches to reach realistic computation of component failure.

References

[1] F. Gallerneau, J.-L. Chaboche, International Journal of Damage Mechanics 8 (1999) 405–427.
[2] A.M. Alam A. Koster, L. Rémy, A physical-base model for life prediction of single crystal turbine blades under creep-fatigue loading and thermal transient conditions, in: L. Rémy, J. Petit (Eds.), Temperature-Fatigue Interaction, ESIS Publication 29, Elsevier, Paris, 2002, pp. 203–212.
[3] N. Marchal, S. Forest, L. Rémy, S. Duvinage, Simulation of fatigue crack growth in single crystal superalloys using local approach to fracture, in: D. Steglich J. Besson, D. Moinereau (Eds.), Local approach to fracture, 9th European Mechanics of Materials Conference, Euromech–Mecamat, Moret–sur–Loing, France, Presses de l'Ecole des Mines de Paris, 2006, pp. 353–358.
[4] J.R. Rice, Mechanics of Materials 6 (1987) 317–335.
[5] S. Flouriot, S. Forest, G. Cailletaud, A. Köster, L. Rémy, B. Burgardt, V. Gros, S. Mosset, J. Delautre, International Journal of Fracture 124 (2003) 43–77.
[6] W. Qi, A. Bertram, International Journal of Plasticity 15 (1999) 1197–1215.
[7] M. Ekh, R. Lillbacka, K. Runesson, International Journal of Plasticity 20 (2004) 2143–2159.
[8] J. Besson, Local approach to fracture, Ecole des Mines de Paris–Les Presses, 2004.
[9] R. Benallal, A. Billardon, G. Geymonat, Some mathematical aspects of the damage softening rate problem, in: D. Steglich J. Besson, D. Moinereau (Eds.), Cracking and Damage, Strain Localization and Size Effect, Crown House, Linton Road, Barking, Essex IG11 8JU, England, Elsevier Science Publishers Ltd., 1988, pp. 247–258.
[10] S. Forest, R. Sievert, International Journal of Solids and Structures 43 (2006) 7224–7245.
[11] N. Marchal, S. Flouriot, S. Forest, L. Remy, Computational Materials Science 37 (2006) 42–50.
[12] Nicolas Marchal, Propagation de fissure en fatigue-fluage á haute température de superalliages monocristallins à base de nickel, Ph.D. Thesis, Ecole des Mines de Paris, 2006.
[13] A.C. Eringen, E.S. Suhubi, International Journal of Engineering Science 2 (1964) 389–404.
[14] S. Forest, The micromorphic approach for gradient elasticity, viscoplasticity and damage, ASCE- Journal of Energy Mechanics, 2008, in press.
[15] R.A.B. Engelen, M.G.D. Geers, F.P.T. Baaijens, International Journal of Plasticity 19 (2003) 403–433.
[16] R. de Borst, Computer Methods in Applied Mechanics and Engineering 103 (1993) 347–362.
[17] S. Forest, R. Sievert, Acta Mechanica 160 (2003) 71–111.
[18] R.H.J. Peerlings, M.G.D. Geers, R. de Borst, W.A.M. Brekelmans, International Journal of Solids Structures 38 (2001) 7723–7746.
[19] R.H.J. Peerlings, T.J. Massart, M.G.D. Geers, Computer Methods in Applied Mechanics and Engineering 193 (2004) 3403–3417.
[20] N. Germain, J. Besson, F. Feyel, Modelling and Simulation in Materials Science and Engineering 15 (2007) S425–S434.
[21] T. Dillard, S. Forest, P. Ienny, European Journal of Mechanics A/Solids 25 (2006) 526–549.